Preoperative Evaluation of Pancreatic Fibrosis and Lipomatosis: Correlation of Magnetic Resonance Findings With Histology Using Magnetization Transfer Imaging and Multigradient Echo Magnetic Resonance Imaging

Schawkat, Khoschy ; Eshmuminov, Dilmurodjon ; Lenggenhager, Daniela ; Endhardt, Katharina ; Vrugt, Bart ; Boss, Andreas ; Petrowsky, Henrik ; Clavien, Pierre-Alain ; Reiner, Caecilia S

Abstract: OBJECTIVES The purpose of this study was to evaluate the diagnostic performance of magnetization transfer (MT) imaging and multigradient echo magnetic resonance imaging (MRI) to quantify pancreatic fibrosis and lipomatosis in patients before pancreatoduodenectomy for postoperative risk stratification with histopathology as the reference standard. MATERIALS AND METHODS Twenty-four patients (age, 68 ± 8 years, 16 males) prospectively underwent quantitative MT imaging using a 2-dimensional gradient echo sequence with and without MT prepulse and multigradient echo imaging on a 3 T MRI 1 day before pancreatoduodenectomy due to adenocarcinoma of the pancreatic head region (n = 20), neuroendocrine tumor (n = 3), or intraductal papillary mucinous neoplasm (n = 1). Magnetization transfer ratio (MTR) and proton density fat fraction (PDFF) were measured in pancreatic tail (PT) and at the resection margin (RM). Histopathologically, pancreatic fibrosis was graded as mild, moderate, or severe (F1-F3), lipomatosis was graded as 0% to 10%, 11% to 30%, and greater than 30% fat deposition (L1-L3). In addition, MTR and histopathologic fibrosis was assessed in pancreatic adenocarcinoma. Mann-Whitney U test and Spearman correlation were used. RESULTS Patients with advanced pancreatic fibrosis (F3) showed a significantly higher MTR compared with the F1 group at the RM and PT (38 ± 4 vs 32.3 ± 1.6, P = 0.018 and 39.7 ± 5.5 vs 31.2 ± 1.7, P = 0.001). Spearman correlation coefficient of MTR and fibrosis grade was r = 0.532 (P = 0.011) and 0.554 (P = 0.008), respectively. Pancreatic parenchyma with advanced fat deposition (L2-L3) showed significantly higher PDFF compared with lipomatosis grade L1 (RM: P = 0.002 and PT: P = 0.001). Proton density fat fraction of pancreatic parenchyma exhibited a moderate and significant correlation with histopathologic lipomatosis grade (RM: r = 0.668 and PT: r = 0.707, P < 0.001). Magnetization transfer ratio was significantly higher in pancreatic adenocarcinoma compared with pancreatic parenchyma (44 ± 5.5 vs 36.0 ± 4.4 and 37.4 ± 5.4, P = 0.004). CONCLUSIONS Multiparametric MRI of the pancreas including MTR and PDFF maps may provide quantitative and noninvasive information on pancreatic fibrosis and lipomatosis before surgery.

DOI: https://doi.org/10.1097/RLI.0000000000000496

Schawkat, Khoschy; Eshmuminov, Dilmurodjon; Lenggenhager, Daniela; Endhardt, Katharina; Vrugt, Bart; Boss, Andreas; Petrowsky, Henrik; Clavien, Pierre-Alain; Reiner, Caecilia S (2018). Preoperative Evaluation of Pancreatic Fibrosis and Lipomatosis: Correlation of Magnetic Resonance Findings With Histology Using Magnetization Transfer Imaging and Multigradient Echo Magnetic Resonance Imaging. Investigative Radiology, 53(12):720-727.
DOI: https://doi.org/10.1097/RLI.0000000000000496

Preoperative Evaluation of Pancreatic Fibrosis and Lipomatosis

Correlation of Magnetic Resonance Findings With Histology Using Magnetization Transfer Imaging and Multigradient Echo Magnetic Resonance Imaging

Khoschy Schawkat, MD, Dilmurodjon Eshmuminov, MD,† Daniela Lenggenhager, MD,‡ Katharina Endhardt, MD,‡ Bart Vrugt, MD,‡ Andreas Boss, MD, PhD,* Henrik Petrowsky, MD,† Pierre-Alain Clavien, MD, PhD,† and Caecilia S. Reiner, MD**

Objectives: The purpose of this study was to evaluate the diagnostic performance of magnetization transfer (MT) imaging and multigradient echo magnetic resonance imaging (MRI) to quantify pancreatic fibrosis and lipomatosis in patients before pancreatoduodenectomy for postoperative risk stratification with histopathology as the reference standard.

Materials and Methods: Twenty-four patients (age, 68 ± 8 years, 16 males) prospectively underwent quantitative MT imaging using a 2-dimensional gradient echo sequence with and without MT prepulse and multigradient echo imaging on a 3 T MRI 1 day before pancreatoduodenectomy due to adenocarcinoma of the pancreatic head region (n = 20), neuroendocrine tumor (n = 3), or intraductal papillary mucinous neoplasm (n = 1). Magnetization transfer ratio (MTR) and proton density fat fraction (PDFF) were measured in pancreatic tail (PT) and at the resection margin (RM). Histopathologically, pancreatic fibrosis was graded as mild, moderate, or severe (F1–F3), lipomatosis was graded as 0% to 10%, 11% to 30%, and greater than 30% fat deposition (L1–L3). In addition, MTR and histopathologic fibrosis was assessed in pancreatic adenocarcinoma. Mann-Whitney *U* test and Spearman correlation were used.

Results: Patients with advanced pancreatic fibrosis (F3) showed a significantly higher MTR compared with the F1 group at the RM and PT (38 ± 4 vs 32.3 ± 1.6, $P = 0.018$ and 39.7 ± 5.5 vs 31.2 ± 1.7, $P = 0.001$). Spearman correlation coefficient of MTR and fibrosis grade was $r = 0.532$ ($P = 0.011$) and 0.554 ($P = 0.008$), respectively. Pancreatic parenchyma with advanced fat deposition (L2–L3) showed significantly higher PDFF compared with lipomatosis grade L1 (RM: $P = 0.002$ and PT: $P = 0.001$). Proton density fat fraction of pancreatic parenchyma exhibited a moderate and significant correlation with histopathologic lipomatosis grade (RM: $r = 0.668$ and PT: $r = 0.707$, $P < 0.001$). Magnetization transfer ratio was significantly higher in pancreatic adenocarcinoma compared with pancreatic parenchyma (44 ± 5.5 vs 36.0 ± 4.4 and 37.4 ± 5.4, $P = 0.004$).

Conclusions: Multiparametric MRI of the pancreas including MTR and PDFF maps may provide quantitative and noninvasive information on pancreatic fibrosis and lipomatosis before surgery.

Key Words: magnetization transfer, proton density fat fraction, pancreatic lipomatosis, pancreatic fibrosis, pancreatic cancer, pancreatoduodenectomy, postoperative pancreatic fistula

(*Invest Radiol* 2018;00: 00–00)

The only potential curative therapy for pancreatic carcinoma at this time is complete surgical resection, which is still associated with a risk for postoperative complications.[1–3] Development of postoperative pancreatic fistula is the most relevant complication with a reported incidence of 10% to 25%[2] and often results in morbidity after pancreatic resection.[4–7] Several factors have been reported to be associated with an increased rate of postoperative pancreatic fistula (POPF), such as pancreatic lipomatosis, absence of fibrosis, and small pancreatic duct size.[4,8–10] Fatty infiltration is thought to increase the softness of the gland and therefore increases the risk of developing POPF.[11,12] Soft pancreas has a high exocrine activity and a poor structure holding capacity leading to technical difficulties with enteropancreatic anastomosis. In opposite, hard pancreatic texture caused by increased fibrosis of the pancreatic tissue is associated with decreased risk of POPF. Fibrotic pancreatic parenchyma has decreased exocrine activity,[9,11,13] which decreases the risk of proteolytic destruction of the anastomosis.[9] Another favorable aspect of fibrosis relates to the increased hardness of the pancreatic texture, which better facilitates the enteropancreatic anastomosis.

Preoperative evaluation of pancreatic parenchyma texture as an indicator of postoperative complications would be of interest for risk stratification of patients and may also influence postoperative patient care or choice of surgical technique. Some studies have attempted to predict the risk of POPF with preoperative magnetic resonance imaging (MRI) by assessing signal characteristics and contrast enhancement of the pancreatic parenchyma as surrogate for pancreatic fibrosis and lipomatosis preoperatively.[4,12,14,15]

Recently, magnetization transfer (MT) MRI has been described as a method to quantify fibrosis.[16] Magnetization transfer describes the physical process of the exchange of magnetization between free hydrogen nuclei and those bound to macromolecules.[15,17,18] The MT effect size depends on the concentrations of these macromolecules, for example, collagen in an aqueous physiological environment,[17] the higher the concentration of macromolecules, the higher the MT effect is. Because the free water proton pool is diminished in a fatty environment, fat deposition in soft tissue environment has a confounding effect on MT ratio (MTR) values. Measured MTR values are reduced in a fatty environment.[17–20] Previous reports showed MT imaging of the small bowel with sufficient image quality for identification of fibrotic scarring in an animal model and in patients with Crohn disease.[17,21] Martens et al[22] used MT imaging to assess tumor response after chemoradiotherapy in rectal cancer with promising results and showed that MTR can be used to discriminate postradiation fibrosis from residual tumor in rectal cancer.[23]

First applications of MT imaging on the pancreas were reported by Li et al,[24] who evaluated MT for quantification of fibrosis levels in pancreatic ductal adenocarcinoma in mouse xenograft models.[19,24] To our best knowledge, this study is the first to describe MT imaging of the pancreas to quantify pancreatic parenchymal fibrosis.

The second component influencing pancreatic texture is pancreatic fat deposition, which can be measured with MRI.[25] In one previous study, a moderate relationship of pancreatic fat fraction obtained with a triple echo gradient echo sequence with histologic findings was found.[4]

The purpose of this study was to evaluate the diagnostic performance of MT imaging and multigradient echo MRI to quantify pancreatic

Received for publication April 14, 2018; and accepted for publication, after revision, May 23, 2018.

From the *Institute of Diagnostic and Interventional Radiology, †Department of Surgery and Transplantation, and ‡Institute of Pathology and Molecular Pathology, University Hospital Zurich, University Zurich, Switzerland.

Conflicts of interest and sources of funding: none declared.

Correspondence to: Caecilia S. Reiner, MD, Institute of Diagnostic and Interventional Radiology, University Hospital Zurich, Raemistrasse 100 8091 Zurich, Switzerland. E-mail: caecilia.reiner@usz.ch.

ISSN: 0020-9996/18/0000–0000
DOI: 10.1097/RLI.0000000000000496

TABLE 1. MRI Parameters of the Magnetization Transfer and Multigradient Echo Sequence

	Magnetization Transfer	Multigradient Echo Sequence
Repetition time, ms	25	9
Echo time, ms	2.17	1.05 2.46 3.69 4.92 6.15 7.38
Field of view, cm	35–43	39–45
Matrix	256 × 208	160 × 140
Bandwidth, Hz	500	1080
Flip angle, degree	20	4
Slice thickness, mm	5	3.5

fibrosis and lipomatosis in patients before pancreatoduodenectomy with histopathology as the reference standard.

MATERIALS AND METHODS

Study Population

The local ethics committee approved this prospective study, and all patients gave written informed consent.

From July 2015 to August 2017, 46 patients were scheduled for pancreatoduodenectomy of a pancreatic head tumor or periampullary tumor and considered for study enrolment. Exclusion criteria were missing informed consent (8 patients) and metallic implants excluding an MR scan (1 patient). Thirty-seven consecutive patients underwent preoperative MR of the pancreas according to the study protocol. Of these 37 patients, 6 patients were excluded because finally no pancreatic resection was performed. Thirty-one patients underwent pancreatoduodenectomy to treat pancreatic, periampullary, or bile duct tumors, and histopathology was assessed for the tumors. In 7 patients, the study-relevant MRI sequences were acquired incompletely. Thus, the remaining 24 patients who had a complete preoperative MR examination and underwent pancreatoduodenectomy were included in this study.

Patients' medical history was assessed (diabetes, prior episodes of pancreatitis, alcohol and nicotine abuses, hypertension, and obesity).

MRI Scan Acquisition

The MR examinations were performed in a 3 T MRI system (Skyra; Siemens Healthcare, Erlangen, Germany) with an 18-channel body array matrix-coil and a built-in 32-channel spine coil. The basic MRI protocol consisted of the following imaging sequences: T2-weighted images coronal and axial, T2-weighted images axial fat-saturated, MR cholangiopancreatography, and noncontrast and dynamic postcontrast T1-weighted axial fat-saturated images. In addition, MT imaging with a 2-dimensional gradient echo sequence and proton density fat fraction (PDFF) mapping with multigradient echo Dixon technique were performed. The off-resonance prepulse of the MT sequence had a Gaussian shape with a frequency offset of 1200 Hz, a maximum effective B1 field of 6.7 μT, a duration of 9984 microseconds, an effective flip angle of 500 degrees, and a bandwidth of 192 Hz. The MRI parameters for the MT sequence and multigradient echo sequence are summarized in Table 1.

Image Analysis

The MTR quantifies the interaction between the unbound water protons and the macromolecular-bound protons and is defined as

$$\mathrm{MTR} = \frac{\mathrm{SI}_0 - \mathrm{SI}_{\mathrm{SAT}}}{\mathrm{SI}_0}$$

where SI_0 and $\mathrm{SI}_{\mathrm{SAT}}$ refer to the image intensity without and with the saturation prepulse, respectively, as earlier described by Pazahr et al.[17] Magnetization transfer ratio values were calculated pixelwise and displayed as MTR maps using an in-house computer script written in Matlab (R2014a; 8.3.0.532). Magnetization transfer ratio measurements were performed on the MTR maps in Matlab. Proton density fat fraction maps were generated by the scanner and analyzed using a DICOM viewing software (Myrian1; Intrasense, Paris, France).

One radiologist (K.S., 5 years of clinical experience) who was blinded to the histopathologic and clinical findings drew regions of interest (ROIs) on MTR maps and PDFF maps. Regions of interest were drawn in nontumorous pancreatic tissue distally located to the tumor avoiding the pancreatic duct and peripancreatic fat with reference of T2-weighted images. One ROI was drawn at the resection margin (RM), and one ROI was drawn in the pancreatic tail (PT), where pancreatic tissue was best visible on the MTR and PDFF maps (Fig. 1). The

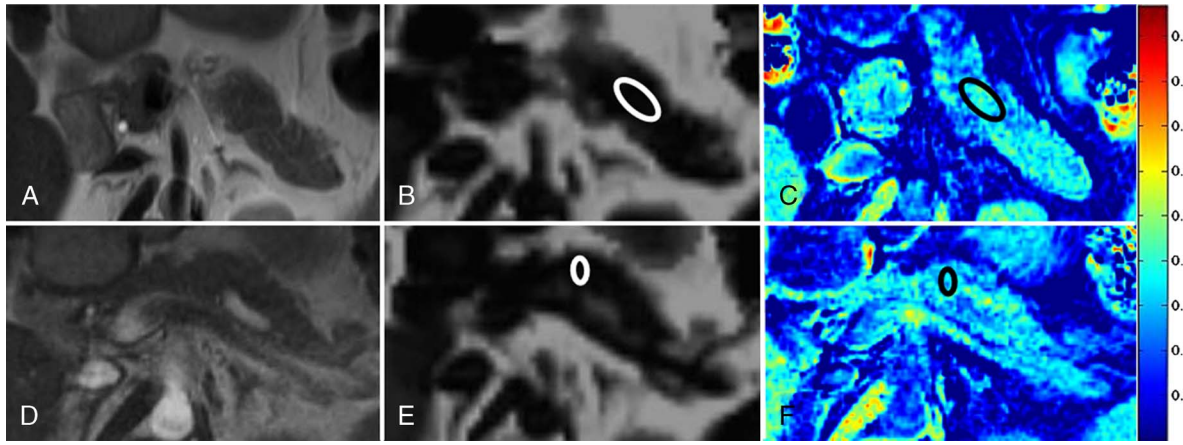

FIGURE 1. A 41-year-old male patient with insulinoma in the pancreatic head. T2 haste axial images show normal pancreatic anatomy at the level of the PT (A) depicting the potential RM (D) without morphologic signs of pancreatic atrophy. Fat fraction measurements using PDFF maps (B and E) show low level of pancreatic lipomatosis (PT, 12.0%; RM, 5.4%) with correlation to histopathology (L1, ≤10%). Magnetization transfer ratio maps were evaluated with corresponding ROI at the PT (C) and RM (F) showing higher grade of pancreatic fibrosis (36.0 and 32.2, respectively) correlating to histopathology (F2, moderate fibrosis).

ROI in the PT was chosen, because in a clinical setting MTR and PDFF would be measured preoperatively in the pancreatic parenchyma and the future RM could not be reliably identified. Therefore, alternative measurements could be more easily performed in the future remaining PT. The RM for each case was identified by the radiologist and pathologist in consensus by matching the surgical specimen and MRI scans using anatomical landmarks (eg, pancreatic groove, portal vein, and superior mesenteric vein) for guidance. In cases with adenocarcinoma in the pancreatic head (14 cases of pancreatic ductal adenocarcinoma and 1 case of distal bile duct adenocarcinoma with the main tumor mass in the pancreatic head), an ROI was manually placed in the pancreatic tumor covering as much as possible of the tumor (avoiding tumor margins) on the axial MT slice with the greatest tumor diameter.

Magnetization transfer ratio values were determined for the skeletal muscle tissue, subcutaneous fat, and the spleen as a reference.

Histopathologic Analysis

The histopathologic features of the pancreatic surgical specimens were evaluated by 2 experienced pathologists in consensus (B.V., 20 years of experience; D.L., 4 years of experience). The histologic analysis consisted of the evaluation of the pancreatic parenchyma at the RM regarding fibrosis and lipomatosis, and the evaluation of desmoplastic fibrosis in the neoplastic lesion. Hematoxylin and eosin staining and elastic van Gieson staining were performed to grade the amount of fibrosis. Hematoxylin and eosin staining was used to grade the degree of fat deposition. For pancreatic fibrosis previously described grading criteria were applied[26]: F0 = normal pancreatic parenchyma, no fibrotic changes; F1 = mild fibrosis with thickening of periductal fibrous tissue; F2 = moderate fibrosis with marked sclerosis of interlobular septa and no evidence of architectural changes; and F3 = severe fibrosis with detection of architectural destruction. For pancreatic lipomatosis, previously described grading criteria[12] were adapted as follows: L1 = 0% to 10% deposition, L2 = 11% to 30%, and L3 = greater than 30%.

Statistical Analysis

Statistical analyses were performed using a commercially available SPSS software Version 22.0.0.0 (IBM Corporation, Armonk, NY). Descriptive statistics were performed on all data and are expressed as mean ± standard deviation (SD). All data were tested for normality using the Kolmogorov-Smirnoff test. Data were analyzed by using Students *t* test to compare MTR and PDFF means for the pancreatic tumor, RM, and the PT.

Mann-Whitney *U* test and analysis of variance (ANOVA) were performed to compare MTR and PDFF means measured in the different histologic fibrosis and lipomatosis groups (F0–F3, L1–L3). Spearman correlation coefficients were obtained for each pair of histologic and MR parameters. Correlation coefficients were interpreted as follows: weak, 0.2; moderate, 0.5; and strong, 0.8.[27] Statistical significance was defined as $P < 0.05$.

RESULTS

Characteristics of the Study Population

Twenty-four patients (mean age, 68 ± 8 years; range, 41–83 years) including 16 men (68 years; range, 41–83 years) and 8 women (69 years; range, 55–79 years) underwent preoperative MRI and pancreatoduodenectomy for adenocarcinoma of the pancreatic head (n = 14), adenocarcinoma of the ampulla vateri (n = 3), duodenal adenocarcinoma (n = 2), adenocarcinoma of the distal bile ducts involving the pancreatic head (n = 1), neuroendocrine tumor (n = 3), and intraductal papillary mucinous neoplasm (n = 1). One patient showed massive parenchymal atrophy disallowing an ROI placement in the pancreatic parenchyma on MT and PDFF sequences, but was included for measuring the MTR in the pancreatic tumor. One patient showed severe artifacts (breathing motion) in the MT sequence and was excluded from MTR measurements.

In total, 22 patients were included for the MTR measurements and 23 patients were included for the PDFF measurements of the pancreatic parenchyma.

The medical history of the included patients revealed that 6 patients had diabetes mellitus type 2, 2 patients had a prior episode of pancreatitis, 2 patients declared alcohol abuse, 3 patients with nicotine abuse, and 14 patients with hypertension. Neither imaging nor histology correlated with these parameters.

Histopathologic Assessment of Pancreatic Fibrosis and Lipomatosis

Histopathologic analysis of the pancreatic parenchyma at the RM revealed 4 patients with F1 fibrosis (18%), 7 patients with F2 fibrosis (32%), and 11 patients with F3 fibrosis (50%). None of the patients had normal (F0) pancreatic parenchyma. Lipomatosis in the pancreatic parenchyma was graded as L1 in 9 patients (39%), L2 in 11 patients (48%), and L3 in 3 patients (13%).

Quantitative Evaluation of MTR Values in the Reference Structures

In the quantitative evaluation of the 2-dimensional MT sequence, we measured high MTR values in reference tissues known to exhibit high MTR: skeletal muscle tissue (48.5% ± 4.0%; n = 24; the erector spinae muscle) and the spleen (36.1% ± 3.4%; n = 18). In the subcutaneous fat, low MTR values were measured (4.0% ± 3.5%; n = 24).

Preoperative MR Assessment of Pancreatic Fibrosis With Magnetization Transfer

The mean MTR at the RM was 36.0 ± 4.4 ($P = 0.004$), and the PT was 37.4 ± 5.4 ($P = 0.004$) and were significantly lower than the mean MTR for the pancreatic tumor (44 ± 5.5, ranged from 32.6 to 53.7; n = 15, all histologic F3) (Fig. 2). Magnetization transfer ratio values at the RM and PT showed moderate correlation with the fibrosis grade (F1–F3) in the specimens ($r = 0.532$, $P = 0.011$ and $r = 0.554$, $P = 0.008$, respectively). Magnetization transfer ratio values for the F3 group were significantly higher compared with the F1 group at the RM and PT (38.0 ± 4.0 vs 32.3 ± 1.6, $P = 0.018$ and 39.7 ± 5.5 vs 31.2 ± 1.7, $P = 0.001$; Fig. 3). Significantly higher MTR values were also found in the F3 group versus F1 + F2 group for measurements at the RM (38.0 ± 4.0 vs 33.9 ± 3.7, $P = 0.023$) and in the F2 versus F1 group in the PT (37.4 ± 3.7 vs 31.2 ± 1.7, $P = 0.014$). Analysis of variance showed significant difference for the mean MTR values of F1 versus F3 group at the RM ($P = 0.013$). Mean MTR values for the fibrosis groups F1 to F3 are summarized in Table 2.

Preoperative MR Assessment of Pancreatic Lipomatosis With Proton Density Fat Fraction

Measured mean and SD PDFF values for the RM and PT were 10% ± 7.5% and 11.1% ± 8% (n = 23). Measured PDFF values at the RM and PT showed moderate correlation with the lipomatosis grade (L1–L3) in the specimens ($r = 0.668$, $P < 0.001$ and $r = 0.707$, $P < 0.001$, respectively). Proton density fat fraction values for the L3 group demonstrated significantly higher values compared with the L1 group for the RM and PT (16.2 ± 5.1 versus 4.1 ± 2.8, $P = 0.012$ and 20.4 ± 6.7 versus 4.8 ± 3.8, $P = 0.009$). Significantly higher PDFF values were also found for the RM and PT comparing L2 versus L1 (13.1 ± 7.8 vs 4.1 ± 2.8, $P = 0.007$; 13.6 ± 7.2 vs 4.8 ± 3.8, $P = 0.005$) (Fig. 4). Analysis of variance showed significant difference for the mean PDFF values of L1 versus L2 group at the RM and PT ($P = 0.009$ and $P = 0.011$, respectively) and for L1 versus L3 ($P = 0.017$ and $P = 0.003$, respectively). Mean PDFF values for the lipomatosis groups L1 to L3 are summarized in Table 2.

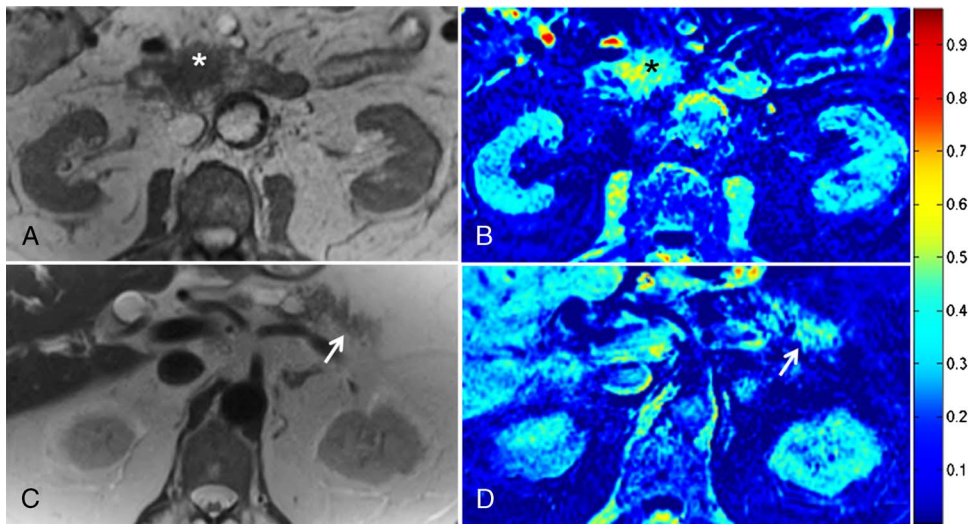

FIGURE 2. A 76-year-old male patient with adenocarcinoma of the pancreatic head. T2 haste axial sequences show a mass in the pancreatic head (A, asterisk) and PT atrophy (C, arrow). Magnetization transfer ratio maps (B and D) demonstrate high-grade fibrosis of the adenocarcinoma in the pancreatic head (B, asterisk) with MTR value of 45.4% ± 7.7% corresponding to desmoplastic reaction in histology and fibrotic changes of the pancreatic parenchyma (D, arrow) with MTR value 39.1% ± 8.2% ($P < 0.001$).

Correlation Between MTR and PDFF

Magnetization transfer ratio values did not show a significant correlation with PDFF values as measured at the RM and in the PT ($r = -0.038$ and $r = -0.131$, $P = 0.867$ and $P = 0.561$, respectively).

No significant correlation was found for the mean MTR values at the RM and the PT and the lipomatosis grade of the specimens ($r = 0.135$, $P = 0.548$ and $r = -0.61$, $P = 0.788$, respectively). Magnetization transfer ratio values did not vary significantly between different lipomatosis groups ($P = 0.276$–0.971, Table 3).

No significant correlation was found for the mean PDFF values at the RM and the PT and the fibrosis grade of the specimens ($r = -0.151$, $P = 0.493$ and $r = -0.219$, $P = 0.316$, respectively). Proton density fat fraction values did not vary significantly between different fibrosis groups ($P = 0.463$–0.989, Table 3).

Analysis of variance showed no significant difference for the amount of lipomatosis in the different fibrosis groups and vice versa (RM: $P = 0.844$ and $P = 0.542$, respectively; PT: $P = 0.724$ and $P = 0.983$, respectively).

DISCUSSION

This study found that advanced pancreatic fibrosis and lipomatosis can be noninvasively quantified with MTR and PDFF MRI. Patients with advanced pancreatic fibrosis or lipomatosis showed significantly higher MTR and PDFF obtained by using MT and multigradient echo MRI. The MR data correlated moderately with histology.

Preoperative quantification of pancreatic fibrosis is of special interest as several studies showed that increased fibrosis of pancreatic tissue is associated with a more secure enteropancreatic anastomosis and

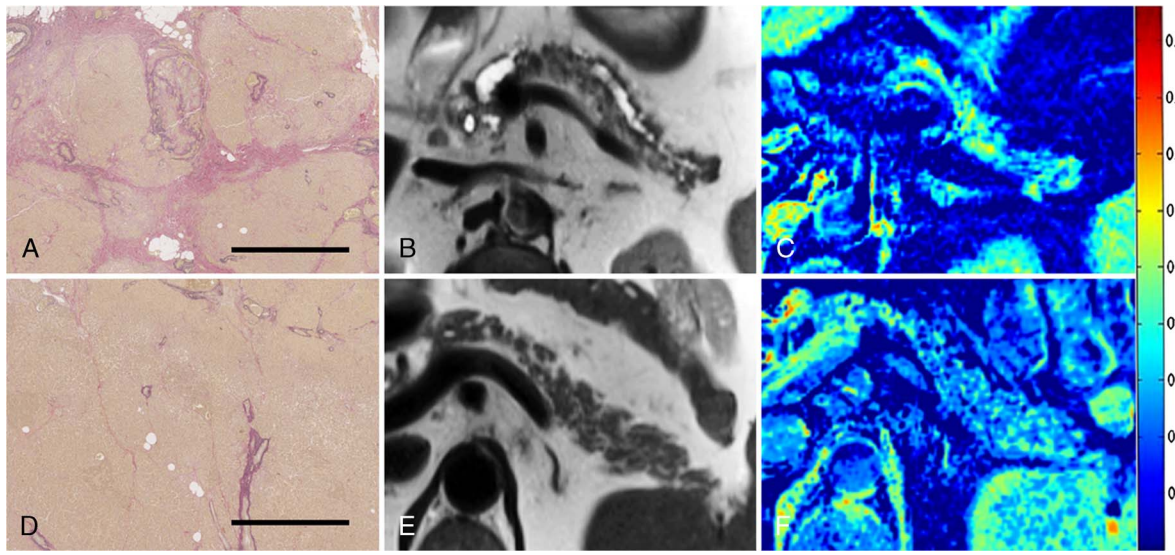

FIGURE 3. In the upper row, an example of a 83-year-old male patient with a neuroendocrine tumor of the papilla vateri is displayed (A, histopathology; B, T2w axial slice; and C, MT sequence axial slice) who shows severe fibrosis in histopathology (F3) with higher MTR values (RM, 39.2% ± 12.1%; PT, 36.9% ± 11.7%) compared with a 67-year-old male patient with adenocarcinoma of the pancreatic head (lower row, D–F) who shows mild fibrosis in histopathology (F1) and lower MTR values (RM, 30% ± 6.3%; PT, 31.2% ± 6.6%). A and D, Elastic van Gieson staining; Scale bar, 1 mm.

TABLE 2. MTR and PDFF Measurements for Different Histopathological Grades of Fibrosis and Lipomatosis

	MTR		PDFF	
	RM	PT	RM	PT
Fibrosis grade				
F1 (n = 4)	32.3 ± 1.6	31.2 ± 1.7	12.1 ± 5.1	14.1 ± 4.2
F2 (n = 7)	34.8 ± 4.5	37.4 ± 3.7	9.5 ± 7.9	10.3 ± 6.7
F3 (n = 11)	38.0 ± 4.0	39.7 ± 5.5	9.5 ± 8.4	10.5 ± 9.8
Lipomatosis grade				
L1 (n = 9)	35.8 ± 3.4	37.7 ± 4.3	4.1 ± 2.8	4.8 ± 3.8
L2 (n = 11)	35.3 ± 4.8	37.3 ± 6.2	13.1 ± 7.8	13.6 ± 7.2
L3 (n = 3)	38.6 ± 5.4	37.1 ± 0.8	16.2 ± 5.1	20.4 ± 6.7

Data are mean ± standard deviation. For pancreatic lipomatosis: L1 = 0%–10% deposition, L2 = 11%–30%, and L3 = greater than 30%.

MTR indicates magnetization transfer ratio; PDFF, proton density fat fraction; RM, resection margin; PT, pancreatic tail; F1, mild fibrosis; F2, moderate fibrosis; and F3, severe fibrosis.

TABLE 3. Analysis of Variance

	Fibrosis		Lipomatosis	
	RM	PT	RM	PT
MTR				
F1 vs F2	0.103	0.551	0.609	0.467
F1 vs F3	0.013	0.050	0.589	0.463
F2 vs F3	0.578	0.232	0.989	0.947
PDFF, %				
L1 vs L2	0.807	0.874	0.009	0.011
L1 vs L3	0.374	0.886	0.017	0.003
L2 vs L3	0.276	0.971	0.707	0.221

Data are P values. $P < 0.05$ indicated a significant difference among the groups. For pancreatic lipomatosis: L1 = 0%–10% deposition, L2 = 11%–30%, and L3 = greater than 30%.

MTR indicates magnetization transfer ratio; PDFF, proton density fat fraction; RM, resection margin; PT, pancreatic tail; F1, mild fibrosis; F2, moderate fibrosis; and F3, severe fibrosis.

less exocrine function.[11,13] Other investigators used the pancreas-to-muscle signal intensity ratio on fat-suppressed T1-weighted MRI scans as a marker for pancreatic fibrosis and showed significant correlation with histology.[12] Yoon et al[4] also used the pancreas-to-muscle signal intensity ratio to quantify pancreatic fibrosis and showed a moderate relationship with histologic finding as patients with advanced fibrosis had significant lower SI ratios than did patients with mild fibrosis. Signal intensity analysis of pancreatic parenchyma on fat-suppressed T1-weighted images, however, may be altered in abnormal parenchyma owing to pancreatic atrophy, fibrosis, edema, or fat deposition, which can be confounding factors. To overcome this problem, we applied an MRI technique based on MT principle to measure pancreatic fibrosis. Physically, MT is a dynamic process that affects spin diffusion between free water molecules and those bound to macromolecules.[19] Thus, MT MRI generates contrast that is primarily determined by the fraction of large macromolecules (eg, in fibrosis) or phospholipid and cell membranes within the interrogated tissue.[19,28,29] As proof of concept, we compared MTR in pancreatic adenocarcinomas, known to exhibit desmoplasia related high-grade fibrosis, with MTR measured in pancreatic parenchyma. We found significantly higher MTR in pancreatic tumor compared with pancreatic parenchyma at the RM and PT. All pancreatic adenocarcinomas showed high-grade desmoplastic fibrosis at histology. This finding is in line with previous studies demonstrating that MT MRI can depict desmoplastic stroma in subcutaneous xenograft mouse tumor models of pancreatic ductal adenocarcinoma and offers the potential of noninvasive quantification of fibrosis levels.[19,24] Furthermore, the MTR values of the pancreatic parenchyma followed the histologic grades of fibrosis with a moderate correlation as well.

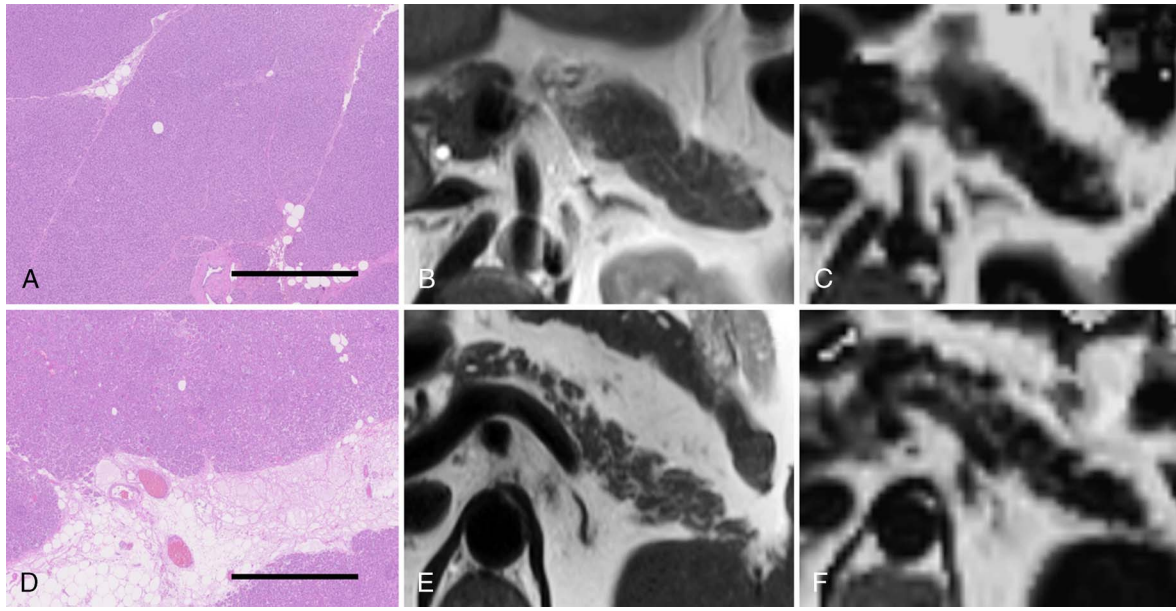

FIGURE 4. In the upper row, an example of a 41-year-old male patient with insulinoma is displayed (A, histopathology; B, T2w axial slice; and C, PDFF sequence axial slice) who shows mild lipomatosis in histopathology (L1 ≤10% fat deposition) with lower PDFF values (RM, 5.4% ± 7.5%; PT, 12% ± 12.7%) compared with a 67-year-old male patient with adenocarcinoma of the pancreatic head (lower row, D–F) who shows higher grade of lipomatosis in histopathology (L2, 11%–30% fat deposition) and higher PDFF values (RM, 10.2% ± 15.5%; PT, 18.4% ± 15.8%). A and D, Hematoxylin and eosin staining; Scale bar, 1 mm.

The MTR values found for the F1 group at the RM were consistently significantly lower than for the F3 group. Magnetization transfer ratio values in the PT were significantly lower in the F1 group than in the F3 group only in the Mann-Whitney *U* test ($P = 0.018$), but not with analysis of variance (marginal *P* value of 0.05). This discordance could be explained by the fact that the histologic fibrosis grades were determined in the pancreatic parenchyma at the RM and are only estimated fibrosis levels of the PT.

The observed MTR values for reference tissues such as skeletal muscle, splenic parenchyma, or subcutaneous fat were in good agreement to previously reported data.[17,30,31]

Although pancreatic fibrosis has been shown to have a positive effect on postoperative outcome after pancreatoduodenectomy, a soft texture related to lipomatosis of the pancreatic parenchyma has been established as a risk factor for fistula development.[3,9,10,32] Lipomatosis can be quantified with a chemical shift-based multiecho gradient imaging sequence using the T2* corrected Dixon technique to measure the PDFF.[33] It divides MRI-visible protons bound to fat by all protons in the parenchyma (bound to fat and water). Fat water separation and T2* signal decay correction is performed by acquires multiple images at different echo times. Several studies proved that MRI-PDFF is a robust and reproducible biomarker for the assessment of nonalcoholic fatty liver disease (NAFLD).[33–37] The research group by Idilman et al[25] applied PDFF to determine pancreatic fat deposition in NAFLD. They report that the mean PDFF values for the pancreatic head, pancreatic body, and PT were 4.6% ± 7.1%, 5.7% ± 6.7%, and 6.6% ± 6.1%, respectively, which is in the same range as the L1 lipomatosis group in our study (mean PDFF values for the RM: 4.1% ± 2.8% and for the PT: 4.8% ± 3.8%). Kühn et al[38] quantified pancreatic fat by PDFF and report similar mean pancreatic fat content not adjusted for potential confounders of pancreatic lipomatosis (ie, body mass index) (head, 4.6%; body, 4.9%; tail, 3.9%; being unequally distributed, $P < 0.001$). Patel et al[39] observed slightly higher PDFF of the pancreas (8.5%) in patients with NAFLD. In our study, the mean PDFF values of the pancreas for all included patients were higher (RM: 10% ± 7.5% and PT: 11% ± 8%). This difference may be potentially explained by the fact that all of our patients had pancreatic head tumors and had a more advanced age compared with the other studies.[25,38,39] Both factors are known to contribute to a higher degree of fatty atrophy of the pancreas.[40–42] The SDs of the PDFF values in our study were relatively high, which is probably due to the low spatial resolution of the PDFF sequence used in this study (Field of view, 39–45 cm; matrix, 160 × 140) and pancreatic atrophy of this study population resulting in a slender residual pancreatic parenchyma disallowing the placement of a large ROI.

In a previous study, Yoon et al[4] estimated pancreatic fat fraction at MRI using T2*-corrected Dixon technique and showed moderate correlation with histology. Although they used a 3-dimensional triple-echo gradient-echo sequence, we investigated a multigradient echo sequence with 6 echoes. A reduced number of echoes may compromise the accuracy for R2* estimation and degrade the noise performance of R2* quantification. However, the optimal number of echoes for PDFF estimation is controversial. Most studies have evaluated a prototype sequence with 6 echoes. Levin et al[43] published results showing that using the 3 or 4 earliest echoes might be of similar or higher accuracy. Zand et al[44] suggest using 3 to 6 echoes to achieve the highest accuracy for hepatic PDFF estimation. A study by Hernando et al[45] propose a minimum number of echoes for robust R2* estimation of 6. Regarding PDFF estimation of the pancreas, so far no data exist comparing the accuracy of 3 or 6 echo techniques. Similar to Yoon et al,[4] we found a moderate correlation of PDFF measurements in the pancreatic parenchyma and histologic grades of lipomatosis. The multigradient echo sequence used in this study does not only accurately quantify pancreatic lipomatosis but would also correct for T2*-decay pronounced in iron deposition in the pancreas.[46] Magnetization transfer in theory would be decreased in the presence of excessive iron overload, but not in limited iron overload.[47] Iron deposition in the pancreas is mainly described in hemochromatosis or thalassemia major. Because we did not have any patients with increased risk of pancreatic iron deposition in our study population, we did not expect any relevant iron deposition in the pancreas. However, in cases of unknown iron deposition, the multigradient echo sequence would correct for the T2*-decay.

In this study, we found no differences in PDFF of the pancreas among patients with different grades of fibrosis. This somehow contradicts the results reported by Yoon et al[4] who found significantly higher fat fractions in patients with advanced fibrosis compared with without or mild fibrosis. However, our PDFF results are accompanied by histopathologic findings, in which no significant differences in grade of lipomatosis were detected between the different fibrosis groups.

Fat deposition in soft tissue environment has a confounding effect on MTR values.[17,18,20,48] The MT effect grows with the number of hydrogen nuclei that switch from a high-mobility environment, such as in a free water molecule, to a low-mobility environment, such as, for example, in a hydroxyl group bound to a macromolecule.[17] The free water proton pool is diminished in a fatty environment and therefore the measured MTR are reduced. Several fat suppression techniques have been applied to remove the fat component from the MT images.[20,49,50] However, fat-suppression and water- or fat-selective pulses may cause additional MT effects and/or alter the steady state of MT sequences.[48] Because the measured PDFF values in this study correlate well with histopathologic grading of the pancreatic lipomatosis, it can be assumed that the applied chemical shift-based multiecho gradient imaging sequence for fat quantification actually measures the fat deposition in the pancreas. Also the MTR measurements in the subcutaneous fat show good agreement with published data with MTR close to zero.[51] Therefore, the applied 2-dimensional gradient echo sequence for fibrosis quantification renders correct quantitative values of MTR in pancreatic tissue also in the case of pancreatic lipomatosis. However, it seems that the lipomatosis of the pancreas in this study population was not pronounced enough to have a reverse effect on the MTR values.

Because of the small patient number, we were not able to adjust our results for patient age. Because patient age is beside fatty atrophy of the pancreas, a risk factor for postoperative pancreatic complications, it should be tested in future and larger studies whether age and level of pancreatic fat as measured by PDFF are independent risk factors.

Our study had also certain limitations. The size of the study cohort and accordingly the subgroups was rather small. Thus, our results should be considered preliminary and require confirmation by studies with larger sample size. Therefore, we performed a retrospective power analysis for comparison of 2 independent means (Student sample *t* test) with continuous values using an alpha of 0.05 and a 2-tailed test. Clinically, a differentiation between high and low to intermediate pancreatic fibrosis (ie, F3 vs F1 + F2) would be of interest for preoperative risk stratification. Magnetization transfer ratio in the PT for F3 (n = 11) in this study was 39.7 ± 5.5 and for F1 + F2 (n = 11) was 34.3 ± 2.7, resulting in a power of 0.847. The same holds true for the differentiation of high to intermediate and low grades of lipomatosis in the PT (ie, L3 + L2 vs L1, respectively). Proton density fat fraction for L3 + L2 (n = 14) in this study was 17 ± 7 and for L1 (n = 9) was 4.8 ± 3.8, resulting in a power of 0.91.

Because patients with normal pancreas or without suspicion of a pancreatic tumor do not undergo biopsy or surgery, they could not be included in this study and are therefore underrepresented. However, it was still feasible to differentiate pancreatic low-grade from high-grade fibrosis with MTR. The clinical impact of high-grade fibrosis as measured with MTR on postoperative patient outcome was not part of this study, because we first aimed to evaluate the diagnostic performance of MT imaging. Future studies with a larger patient cohort should focus on prediction of postoperative patient outcome based on MT measurements of pancreatic fibrosis. Because of the small patient number, we

were not able to adjust our results for patient age. Because patient age is beside fatty atrophy of the pancreas a risk factor for postoperative pancreatic complications, it should be tested in future and larger studies whether age and level of pancreatic fat as measured by PDFF are independent risk factors. In addition, patients included in the study presented a variety of pancreatic tumors such as adenocarcinomas as the largest subgroup as well as intraductal papillary mucinous neoplasm and neuroendocrine tumors. Different pancreatic cancer etiologies may have also different effects on the composition of residual pancreatic parenchyma. Because we obtained all data with the same MR scanner, studies including multiple imagers from various vendors are warranted. Regarding different field strength, MTR values vary only slightly between 1.5 T and 3.0 T.[52] Finally, the current study was performed with ROI-based measurements that encompassed the pancreatic tissue within one slice for both MRI and histology measurements. This associated with challenges in coregistration of histology slides to corresponding in vivo MRI measurements. The imprecision associated with this manual analysis along with the significant difference between MRI slice thickness (millimeter) and histology tissue slice thickness (micrometer) may have been a key source for the variability between MRI and histologic measurements.

In conclusion, multiparameteric MRI of the pancreas including MTR and PDFF maps may provide noninvasive information to quantify pancreatic fibrosis and lipomatosis before pancreatic surgery. Further studies are needed to investigate whether MTR and PDFF may serve as an imaging marker to noninvasively estimate the risk of postoperative complications associated with pancreatic fibrosis and lipomatosis.

REFERENCES

1. Chari ST, Kelly K, Hollingsworth MA, et al. Early detection of sporadic pancreatic cancer: summative review. *Pancreas*. 2015;44:693.
2. Cuellar E, Muscari F, Tuyeras G, et al. Use of routine CT-SCANS to detect severe postoperative complications after pancreato-duodenectomy. *J Visc Surg*. 2017.
3. Yeo CJ, Cameron JL, Maher MM, et al. A prospective randomized trial of pancreaticogastrostomy versus pancreaticojejunostomy after pancreaticoduodenectomy. *Ann Surg*. 1995;222:580–588; discussion 8–92.
4. Yoon JH, Lee JM, Lee KB, et al. Pancreatic steatosis and fibrosis: quantitative assessment with preoperative multiparametric MR imaging. *Radiology*. 2016;279:140–150.
5. Brient C, Regenet N, Sulpice L, et al. Risk factors for postoperative pancreatic fistulization subsequent to enucleation. *J Gastrointest Surg*. 2012;16:1883–1887.
6. Butturini G, Daskalaki D, Molinari E, et al. Pancreatic fistula: definition and current problems. *J Hepatobiliary Pancreat Surg*. 2008;15:247–251.
7. Vin Y, Sima CS, Getrajdman GI, et al. Management and outcomes of postpancreatectomy fistula, leak, and abscess: results of 908 patients resected at a single institution between 2000 and 2005. *J Am Coll Surg*. 2008;207:490–498.
8. Kirihara Y, Takahashi N, Hashimoto Y, et al. Prediction of pancreatic anastomotic failure after pancreatoduodenectomy: the use of preoperative, quantitative computed tomography to measure remnant pancreatic volume and body composition. *Ann Surg*. 2013;257:512–519.
9. Mathur A, Pitt HA, Marine M, et al. Fatty pancreas: a factor in postoperative pancreatic fistula. *Ann Surg*. 2007;246:1058–1064.
10. Yang YM, Tian XD, Zhuang Y, et al. Risk factors of pancreatic leakage after pancreaticoduodenectomy. *World J Gastroenterol*. 2005;11:2456–2461.
11. Uchida E, Tajiri T, Nakamura Y, et al. Relationship between grade of fibrosis in pancreatic stump and postoperative pancreatic exocrine activity after pancreaticoduodenectomy: with special reference to insufficiency of pancreaticointestinal anastomosis. *J Nippon Med Sch*. 2002;69:549–556.
12. Watanabe H, Kanematsu M, Tanaka K, et al. Fibrosis and postoperative fistula of the pancreas: correlation with MR imaging findings—preliminary results. *Radiology*. 2014;270:791–799.
13. Friess H, Malfertheiner P, Isenmann R, et al. The risk of pancreaticointestinal anastomosis can be predicted preoperatively. *Pancreas*. 1996;13:202–208.
14. Dinter DJ, Aramin N, Weiss C, et al. Prediction of anastomotic leakage after pancreatic head resections by dynamic magnetic resonance imaging (dMRI). *J Gastrointest Surg*. 2009;13:735–744.
15. Kim Z, Kim MJ, Kim JH, et al. Prediction of post-operative pancreatic fistula in pancreaticoduodenectomy patients using pre-operative MRI: a pilot study. *HPB (Oxford)*. 2009;11:215–221.
16. Jiang K, Ferguson CM, Woollard JR, et al. Magnetization transfer magnetic resonance imaging noninvasively detects renal fibrosis in swine atherosclerotic renal artery stenosis at 3.0 T. *Invest Radiol*. 2017;52:686–692.
17. Pazahr S, Blume I, Frei P, et al. Magnetization transfer for the assessment of bowel fibrosis in patients with Crohn's disease: initial experience. *MAGMA*. 2013;26:291–301.
18. Rosenkrantz AB, Storey P, Gilet AG, et al. Magnetization transfer contrast-prepared MR imaging of the liver: inability to distinguish healthy from cirrhotic liver. *Radiology*. 2012;262:136–143.
19. Li W, Zhang Z, Nicolai J, et al. Quantitative magnetization transfer MRI of desmoplasia in pancreatic ductal adenocarcinoma xenografts. *NMR Biomed*. 2013;26:1688–1695.
20. Smith AK, Dortch RD, Dethrage LM, et al. Incorporating dixon multi-echo fat water separation for novel quantitative magnetization transfer of the human optic nerve in vivo. *Magn Reson Med*. 2017;77:707–716.
21. Adler J, Swanson SD, Schmiedlin-Ren P, et al. Magnetization transfer helps detect intestinal fibrosis in an animal model of Crohn disease. *Radiology*. 2011;259:127–135.
22. Martens MH, Lambregts DM, Papanikolaou N, et al. Magnetization transfer imaging to assess tumour response after chemoradiotherapy in rectal cancer. *Eur Radiol*. 2016;26:390–397.
23. Martens MH, Lambregts DM, Papanikolaou N, et al. Magnetization transfer ratio: a potential biomarker for the assessment of postradiation fibrosis in patients with rectal cancer. *Invest Radiol*. 2014;49:29–34.
24. Li W, Zhang Z, Nicolai J, et al. Magnetization transfer MRI in pancreatic cancer xenograft models. *Magn Reson Med*. 2012;68:1291–1297.
25. Idilman IS, Tuzun A, Savas B, et al. Quantification of liver, pancreas, kidney, and vertebral body MRI-PDFF in non-alcoholic fatty liver disease. *Abdom Imaging*. 2015;40:1512–1519.
26. Wellner UF, Kayser G, Lapshyn H, et al. A simple scoring system based on clinical factors related to pancreatic texture predicts postoperative pancreatic fistula preoperatively. *HPB (Oxford)*. 2010;12:696–702.
27. Zou KH, Tuncali K, Silverman SG. Correlation and simple linear regression. *Radiology*. 2003;227:617–622.
28. Henkelman RM, Stanisz GJ, Graham SJ. Magnetization transfer in MRI: a review. *NMR Biomed*. 2001;14:57–64.
29. Wolff SD, Balaban RS. Magnetization transfer contrast (MTC) and tissue water proton relaxation in vivo. *Magn Reson Med*. 1989;10:135–144.
30. Boss A, Martirosian P, Kuper K, et al. Whole-body magnetization transfer contrast imaging. *J Magn Reson Imaging*. 2006;24:1183–1187.
31. Stanisz GJ, Odrobina EE, Pun J, et al. T1, T2 relaxation and magnetization transfer in tissue at 3T. *Magn Reson Med*. 2005;54:507–512.
32. Gaujoux S, Cortes A, Couvelard A, et al. Fatty pancreas and increased body mass index are risk factors of pancreatic fistula after pancreaticoduodenectomy. *Surgery*. 2010;148:15–23.
33. Idilman IS, Aniktar H, Idilman R, et al. Hepatic steatosis: quantification by proton density fat fraction with MR imaging versus liver biopsy. *Radiology*. 2013;267:767–775.
34. Dulai PS, Sirlin CB, Loomba R. MRI and MRE for non-invasive quantitative assessment of hepatic steatosis and fibrosis in NAFLD and NASH: Clinical trials to clinical practice. *J Hepatol*. 2016;65:1006–1016.
35. Permutt Z, Le TA, Peterson MR, et al. Correlation between liver histology and novel magnetic resonance imaging in adult patients with non-alcoholic fatty liver disease—MRI accurately quantifies hepatic steatosis in NAFLD. *Aliment Pharmacol Ther*. 2012;36:22–29.
36. Tang A, Tan J, Sun M, et al. Nonalcoholic fatty liver disease: MR imaging of liver proton density fat fraction to assess hepatic steatosis. *Radiology*. 2013;267:422–431.
37. Eshmuminov D, Tschuor C, Raptis DA, et al. Rapid liver volume increase induced by associating liver partition with portal vein ligation for staged hepatectomy (ALPPS): Is it edema, steatosis, or true proliferation? *Surgery*. 2017;161:1549–1552.
38. Kühn JP, Berthold F, Mayerle J, et al. Pancreatic steatosis demonstrated at MR imaging in the general population: clinical relevance. *Radiology*. 2015;276:129–136.
39. Patel N, Peterson M, Brenner D, et al. Association between novel MRI-estimated pancreatic fat and liver histology-determined steatosis and fibrosis in non-alcoholic fatty liver disease. *Aliment Pharmacol Ther*. 2013;37:630–639.
40. Matsuda Y. Age-related pathological changes in the pancreas. *Front Biosci (Elite Ed)*. 2018;10:137–142.
41. Wang H, Maitra A, Wang H. Obesity, intrapancreatic fatty infiltration, and pancreatic cancer. *Clin Cancer Res*. 2015;21:3369–3371.

42. Schawkat K, Kuhn W, Inderbitzin D, et al. Diagnostic value and interreader agreement of the pancreaticolienal gap in pancreatic cancer on MDCT. *PLoS One*. 2016;11:e0166003.
43. Levin YS, Yokoo T, Wolfson T, et al. Effect of echo-sampling strategy on the accuracy of out-of-phase and in-phase multiecho gradient-echo MRI hepatic fat fraction estimation. *J Magn Reson Imaging*. 2014;39:567–575.
44. Zand KA, Shah A, Heba E, et al. Accuracy of multiecho magnitude-based MRI (M-MRI) for estimation of hepatic proton density fat fraction (PDFF) in children. *J Magn Reson Imaging*. 2015;42:1223–1232.
45. Hernando D, Kramer JH, Reeder SB. Multipeak fat-corrected complex R2* relaxometry: theory, optimization, and clinical validation. *Magn Reson Med*. 2013;70:1319–1331.
46. Fukuzawa K, Hayashi T, Takahashi J, et al. Evaluation of six-point modified dixon and magnetic resonance spectroscopy for fat quantification: a fat-water-iron phantom study. *Radiol Phys Technol*. 2017;10:349–358.
47. Salustri C. Lack of magnetization transfer from the ferritin molecule. *J Magn Reson B*. 1996;111:171–173.
48. Li W, Wang X, Miller FH, et al. Chemical Shift magnetization transfer magnetic resonance imaging. *Magn Reson Med*. 2017;78:656–663.
49. Kaldoudi E, Williams SC, Barker GJ, et al. A chemical shift selective inversion recovery sequence for fat-suppressed MRI: theory and experimental validation. *Magn Reson Imaging*. 1993;11:341–355.
50. Dwyer AJ, Frank JA, Sank VJ, et al. Short-Ti inversion-recovery pulse sequence: analysis and initial experience in cancer imaging. *Radiology*. 1988;168:827–836.
51. Loesberg AC, Kormano M, Lipton MJ. Magnetization transfer imaging of normal and abnormal liver at 0.1 T. *Invest Radiol*. 1993;28:726–731.
52. Martirosian P, Boss A, Deimling M, et al. Systematic variation of off-resonance prepulses for clinical magnetization transfer contrast imaging at 0.2, 1.5, and 3.0 tesla. *Invest Radiol*. 2008;43:16–26.